The effects of alpha-radiolysis on UO_2 dissolution determined from batch experiments with ^{238}Pu-doped UO_2

S. Stroes-Gascoyne [a,*], F. Garisto [b], J.S. Betteridge [a]

[a] *Atomic Energy of Canada Limited, Whiteshell Laboratories, Pinawa, Man., Canada R0E 1L0*
[b] *Ontario Power Generation, Toronto, Ont., Canada*

Abstract

The effects of alpha dose-rate on UO_2 dissolution were investigated by performing dissolution experiments with ^{238}Pu-doped UO_2 materials containing nominal alpha-activity levels of $\sim$1–100 Ci/kg UO_2 (actual levels 0.4–80 Ci/kg UO_2), in 0.1 M $NaClO_4$ and in 0.1 M $NaClO_4$ + 0.1 M carbonate. Dissolution rates increased less than 10-fold for an almost 100-fold increase in doping level and fall within the range of predictions of the Mixed Potential Model (a detailed mechanistic model for used fuel dissolution). Dissolution rates were lower in carbonate-free solutions and enrichment of ^{238}Pu on the UO_2 surface was suggested in carbonate solutions. Effective G values, defined as the ratio of the total amount of U dissolved divided by the maximum possible amount of U dissolved by radiolytically produced H_2O_2, increased with decreasing doping levels. This suggests that the dissolution reaction at high dose rates is limited by the reaction rate between UO_2 and H_2O_2, but becomes increasingly limited by the rate of production of H_2O_2 at lower dose rates.
© 2005 Published by Elsevier B.V.

1. Introduction

In a geologic repository for used nuclear fuel, the long-term stability of the fuel will be determined by the influence of α-radiolysis, since the dose-rate for α-radiolysis will exceed that for γ/β-radiolysis beyond a fuel age of $\sim$200 years and will persist for more than 10 000 years [1]. However, since 200-year old spent fuel is not available at present, it is not possible to exclude γ/β radiolysis effects from experiments conducted with spent fuel and any dissolution rates derived from such studies necessarily incorporate radiolysis effects from γ/β- as well as α-radiolysis.

The use of external α-sources [2–4], and chemically added H_2O_2 (as a surrogate for radiolytically produced oxidants [5]) in electrochemical experiments have provided much information on the basic chemistry/electrochemistry of α-radiolysis effects on UO_2 fuel dissolution. Recent corrosion potential (E_{corr}) measurements obtained with ^{238}Pu-doped UO_2 electrodes [6] and published E_{corr} data obtained with UO_2 electrodes in the presence of external alpha sources [2] were compared. Results showed that the E_{corr} values for ^{238}Pu-doped electrodes were similar to the published values obtained

* Corresponding author. Tel.: +1 204 753 2311; fax: +1 204 753 2690.
E-mail address: stroesgascoynes@aecl.ca (S. Stroes-Gascoyne).

with undoped UO_2 electrodes, for the same alpha source strengths [7].

Other international laboratories have carried out dissolution experiments with α-doped UO_2 in N_2-degassed demineralised water. Rondinella et al. [8] have measured uranium release rates from UO_2 pellets that were doped uniformly (using a sol–gel precipitation method) with either 0.1 or 10 wt% of the α-emitter ^{238}Pu. Results showed that the amount of uranium released by dissolution was only approximately one order of magnitude greater than the amount released from an undoped pellet. Similar trends were found in subsequent experiments with crushed (higher surface area) samples [9]. The release rate measured by Rondinella et al. [8] was approximately the same as that determined for unirradiated UO_2 in aerated demineralised water.

This paper describes the results from dissolution experiments with ^{238}Pu-doped materials. The experiments were performed to obtain data to further validate results from the Mixed Potential Model (MPM). The MPM for used fuel dissolution was first developed in 1998, and is based on a detailed (electrochemical) mechanistic model of used UO_2 fuel dissolution, developed from the wealth of experimental electrochemical data measured on UO_2 at the Whiteshell Laboratories over the past ∼15 years [1,10,11].

The MPM has been used to predict the effects of alpha-radiolysis, precipitation and redox reactions with Fe(II) on used fuel dissolution [12–14]. The MPM has also been used to predict the effect of the carbon steel container components on used fuel dissolution [15]. Recently, MPM predictions have been compared with various independently obtained national and international experimental data (including both electrochemical E_{corr} values and UO_2 dissolution rates) in an attempt to validate the MPM [16]. The initial E_{corr} data measured with ^{238}Pu-doped UO_2 electrodes [6] were also included in the verification. Results suggested that the MPM predictions are generally in good agreement with experimental observations, especially under more oxidizing conditions. The MPM tends to overestimate both the E_{corr} and dissolution rate under mildly oxidizing conditions, as a consequence of using interfacial rate constants derived from data obtained under oxidizing conditions, and the fact that the surface reactivity of UO_2 appears to decrease with decreasing potential. In a recent sensitivity analysis, it was determined that the interfacial rate constant for the reduction of H_2O_2 on UO_2 was the most important factor affecting the effective G-values (G_{eff}, defined as the ratio of the total amount of U dissolved divided by the maximum possible amount of U dissolved by radiolytically produced H_2O_2) predicted by the MPM [17]. More experimental data are needed to narrow down the range of uncertainty in the interfacial rate constant for the reduction of H_2O_2 on UO_2, estimated by King and Kolar [17] to be up to six orders of magnitude.

2. Experimental approach

2.1. Fabrication of ^{238}Pu-doped material

The fabrication of the ^{238}Pu-doped material has been described elsewhere in detail [18]. Briefly, (slightly depleted) UO_2 powder was thoroughly mixed for 30 min with high-purity $^{238}PuO_2$ (>99.2% ^{238}Pu) in a (new, uncontaminated) Pilmac Vibratory mill, followed by pressing and sintering of the pellets for 2 h at 1650 °C in a dilute hydrogen cover gas (10% H_2/90% N_2). Geometric densities of the pellets were typically 10.3–10.4 g/cm³ but no porosity measurements were made [18]. After the pellets were cut into 3-mm thick discs and the discs used to make electrodes for a different study, it was noticed that the electrical conductivity of the materials was lower than desired. This suggested that the materials were slightly hypostoichiometric, possibly due to the reduction of Pu(IV) to Pu(III) during sintering.

All materials were, therefore, re-heated at 1000 °C for 24 h in the presence of a small amount of O_2 (i.e., oxygen pressure of about 2.7×10^{-15} atm. [18]) in order to induce a slight hyperstoichiometry (i.e., $UO_{2.00x}$, × not measured) and improve the conductivity of the materials so that electrodes could be made.

The materials prepared contained nominally about 1, 10 and 100 Ci/kg UO_2 (0.006, 0.06 and 0.6 wt% ^{238}Pu). Typical used CANDU fuel with a burnup of 685 GJ/kg contains ∼1 Ci/kg UO_2 of α-activity, after about 30 years cooling. Undoped pellets were also prepared specifically for this study from the same (slightly depleted) UO_2 powder, using the same mixing, pressing and sintering procedures.

2.2. Dissolution experiments

The dissolution behaviour of these materials (and the undoped UO_2) was investigated to determine the effects of α-dose-rate, precipitation and time on the dissolution of UO_2. The effect of precipitation was studied by carrying out the dissolution experiments in perchlorate solution (0.1 M $NaClO_4$) and perchlorate/carbonate solution (0.1 M $NaClO_4$ + 0.1 M carbonate (0.03 M Na_2CO_3 and 0.07 M $NaHCO_3$)) at pH 9.5. (This carbonate concentration is much higher than would be encountered in a deep geologic repository and is used solely to ensure the effects of carbonate are measurable.) The time dependence of the dissolution rate was investigated by carrying out Experiment 1 for 167 days and a duplicate Experiment 2 for 270 days.

Preparation of the undoped UO_2 and ^{238}Pu-doped UO_2 materials for the dissolution experiments involved polishing the 3-mm thick discs on 600 grit wetted silicone carbide paper (to remove oxidized material), rinsing with distilled deionized water (to remove fines) and pre-leaching for 24 h in 100 ml Ar-deaerated perchlorate

or perchlorate/carbonate solutions (to remove any remaining fines or oxidized material from the UO_2 surfaces). After 24 h, each disc was removed from the pre-leach solution and rinsed. The discs were then placed immediately in small, tightly capped, glass bottles containing 20 ml fresh Ar-deaerated solutions, and leached for 167 or 270 days. At the end of the experiments, the UO_2 discs were removed from solution and the amount of U and Pu dissolved was determined from solution analysis (after a minimum 2-h acidification of the solutions with 10% nitric acid in the glass bottles to include any U and Pu in colloidal form or adsorbed on vessel walls). The amount and composition of any surface precipitate on the UO_2 discs was assessed by exposure to 60 s dips in 0.1 M HCl, followed by solution analysis. Pu isotopes were separated by optimized solvent extraction procedures and quantified by alpha-spectroscopy. Uranium concentrations were determined by inductively coupled plasma mass spectrometry (ICP-MS).

Because the ^{238}Pu-doped material was prepared by mechanically mixing PuO_2 and UO_2 powders, it is assumed that the materials consist of islands of PuO_2 embedded in a sea of UO_2, i.e., most Pu is not dissolved in the UO_2 matrix. Thus, since this material is morphologically different from CANDU used fuel, the behaviour of Pu observed in these dissolution experiments is not necessarily the same as would be observed for CANDU used fuel. In particular, Pu and U can dissolve independently from each other whereas, for CANDU fuel, Pu is only released as the UO_2 matrix dissolves. However, the effects of alpha-radiolysis on uranium behaviour should be similar for the nominal 1 Ci/kg UO_2 material and >200 year old CANDU used fuel (i.e., after the fuel's γ/β-fields have decayed and radiolytic oxidants are produced mainly by α-radiolysis).

2.3. Nominal versus actual composition of the ^{238}Pu-doped material

The nominal compositions of the ^{238}Pu-doped materials were about 1, 10 and 100 Ci/kg UO_2. Because these materials were fabricated using a mechanical mixing procedure, there was some concern over the actual composition of these materials and their microscopic homogeneity. In order to determine the actual bulk composition of these materials, one quarter of a 3-mm thick disc of each material (including the undoped material) was dissolved in 100 ml concentrated HNO_3 containing 0.05 M HF. Thermal ionization mass spectrometry (TIMS) was used to analyze these acid solutions for U and Pu.

3. Results

Table 1 compares the actual U/^{238}Pu mass ratios and activity levels (in Ci/kg UO_2) in the materials, as measured from the dissolution of quarter discs of the materials, with the nominal values.

Fig. 1 shows the mass of U leached (in μg) from the UO_2 discs after 24 h, 176 d and 270 d.

Fig. 2 shows the mass of precipitated U (determined from the 60 s dips in 0.1 M HCl) on the various UO_2 surfaces after 167 d and 270 d. Table 2 gives dissolution rates, calculated from the total amount of U dissolved (see Figs. 1 and 2), the geometric surface area (SA) of the discs and the leach time.

Figs. 3 and 4 show uranium enrichment ratios (UER's) for Experiments 1 and 2. A UER is the measured U/^{238}Pu mass ratio in solution (or on the UO_2 surface) divided by the actual U/^{238}Pu ratio in the solid. A UER = 1 indicates congruent dissolution of U and Pu, a UER >1 suggests U solution (or surface) enrichment, whereas a UER < 1 indicates Pu solution (or surface) enrichment. The UER values in Figs. 3 and 4 are calculated with the measured U/^{238}Pu ratios (Table 1).

Table 3 gives the calculated G_{eff} values. The amount of radiolytically produced H_2O_2 (the primary oxidant generated by alpha radiolysis [19]) needed for the calculation of G_{eff} was determined from the measured doping levels, the leach times, the geometric surface areas of the UO_2 discs and the primary H_2O_2 G-value (0.985 molecules/100 eV) for alpha-radiolysis. Details of this calculation are given in Ref. [6].

4. Discussion

4.1. Actual composition of the materials

The U/^{238}Pu mass ratio results in Table 1 show that the actual compositions of the ^{238}Pu-doped materials

Table 1

Comparison of measured and nominal U/^{238}Pu mass ratios and alpha activities in the ^{238}Pu-doped materials

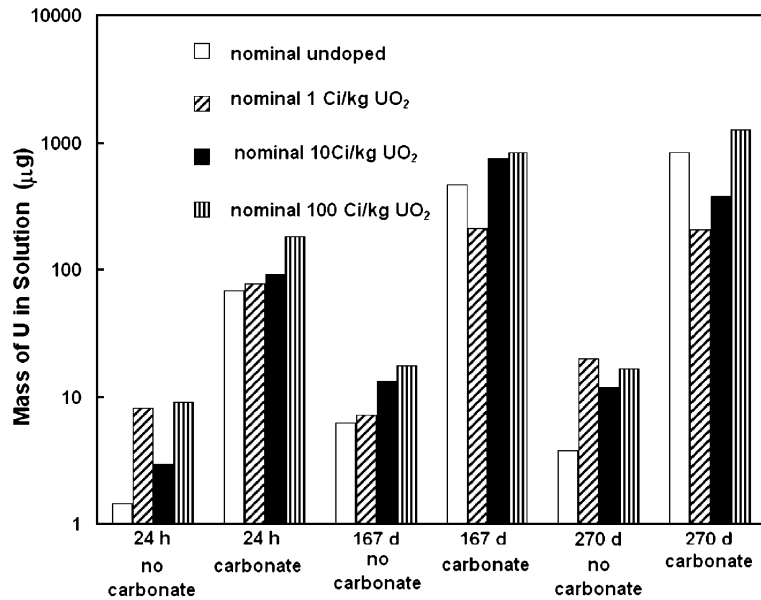| Material (Ci/kg UO_2)	U/^{238}Pu mass ratio measured	U/^{238}Pu mass ratio nominal	Alpha activity measured (Ci/kg UO_2)	Alpha activity nominal (Ci/kg UO_2)
100	190 ± 0.5%	155	80.0 ± 0.4%	100
10	1200 ± 0.7%	1550	12.5 ± 0.4%	10
1	7030 ± 0.7%	15 500	2.2 ± 0.5%	1
0	N/A	N/A	0.4 ± 0.5%	0

Fig. 1. Mass of U leached into solution for the pre-leach (24 h), the 167 d and 270 d experiments.
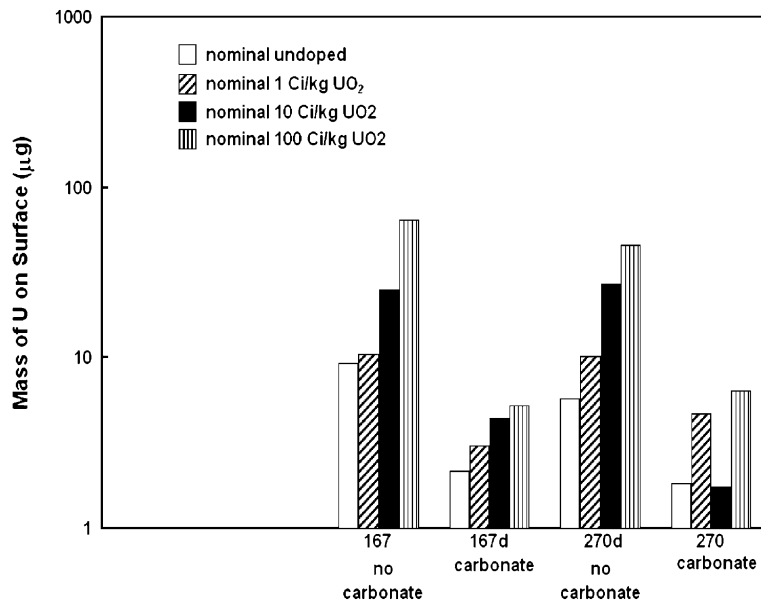

Fig. 2. Mass of U precipitated on the [238]Pu-doped UO_2 surfaces for the 167 d and 270 d experiments.

differ from the nominal values. The difference in the actual and nominal compositions of the 100 and 10 Ci/kg UO_2 materials is −20% and +25%, respectively, but for the nominal 1 Ci/kg UO_2 material the difference is +220%. Also, the undoped material contains about 0.4 Ci/kg UO_2 alpha-activity.

The cause of these differences must be sought in the manner these materials were made [18]. The most con-

centrated material was made first by mechanically mixing about 250 mg [238]Pu (as [238]PuO_2) and about 44 g powdered UO_2 in a new, uncontaminated Pilmac Vibratory mill for 30 min. Ninety percent of this first mix (nominal 100 Ci/kg UO_2) was removed from the mill and more UO_2 was added to make the next activity level (nominal 10 Ci/kg UO_2). This process was repeated a third time to make the nominal 1 Ci/kg UO_2 material.

Table 2
Dissolution rates after 167 and 270 days of leaching

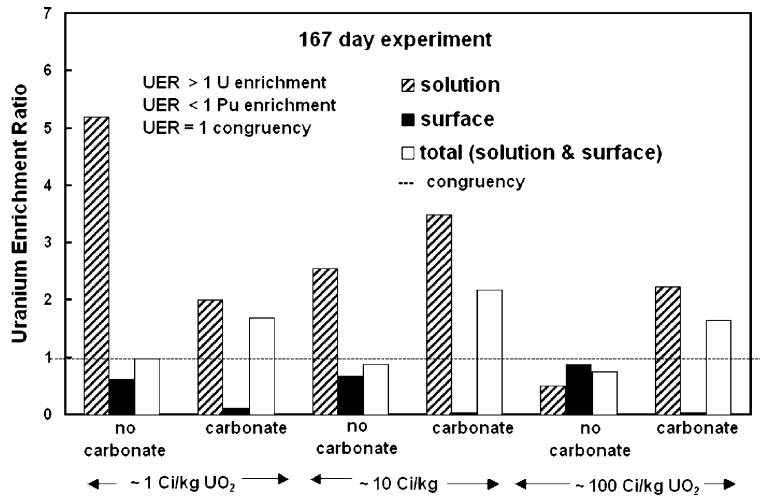| UO$_2$ sample (Ci/kg UO$_2$)	0.1 M carbonate present	Experiment 1: 167 days			Experiment 2: 270 days		
		SA[a] of UO$_2$ (cm^2)	U total (in solution + on surface) (µg)	U dissolution rate (µg/cm^2 s)	SA[a] of UO$_2$ (cm^2)	U total (in solution + on surface) (µg)	U dissolution rate (µg/cm^2 s)
1	−	2.59	17.8 ± 3%	$4.8 \times 10^{-7} \pm 3\%$	3.10	30.6 ± 8%	$4.2 \times 10^{-7} \pm 8\%$
1	+	2.88	214 ± 5%	$5.1 \times 10^{-6} \pm 5\%$	2.87	213 ± 10%	$3.2 \times 10^{-6} \pm 10\%$
10	−	2.74	38.4 ± 3%	$9.7 \times 10^{-7} \pm 3\%$	2.53	38.9 ± 7%	$6.6 \times 10^{-7} \pm 7\%$
10	+	2.93	760 ± 4%	$1.8 \times 10^{-5} \pm 4\%$	2.69	380 ± 7%	$6.1 \times 10^{-6} \pm 7\%$
100	−	2.65	82.0 ± 3%	$2.1 \times 10^{-6} \pm 3\%$	2.73	62.7 ± 6%	$9.9 \times 10^{-7} \pm 6\%$
100	+	2.53	842 ± 6%	$2.3 \times 10^{-5} \pm 6\%$	3.08	1280 ± 11%	$1.8 \times 10^{-5} \pm 11\%$
0	−	2.66	15.5 ± 3%	$4.0 \times 10^{-7} \pm 3\%$	2.77	9.6 ± 14%	$1.5 \times 10^{-7} \pm 14\%$
0	+	2.95	467 ± 5%	$1.1 \times 10^{-5} \pm 5\%$	2.83	839 ± 10%	$1.3 \times 10^{-5} \pm 10\%$

[a] SA = geometric surface area.

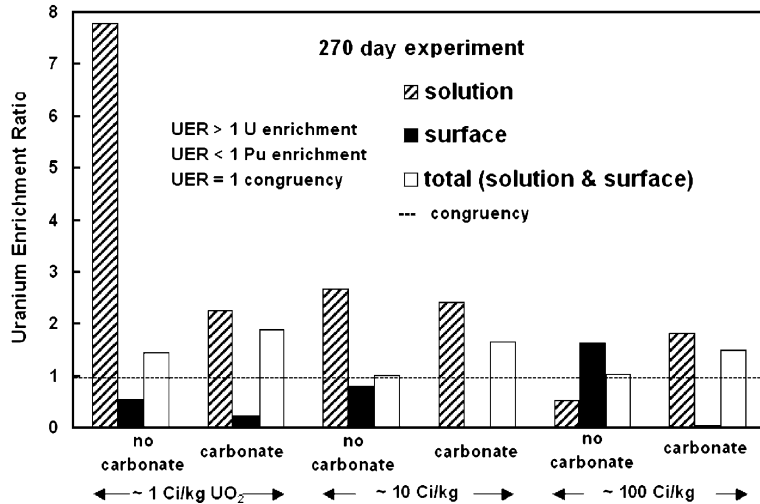
Fig. 3. Uranium enrichment ratios for the 167 d experiment.

Fig. 4. Uranium enrichment ratios for the 270 d experiment.

Table 3
G_{eff} values calculated from dissolution data

UO$_2$ sample (Ci/kg UO$_2$)	0.1 M carbonate present	Geometric SA of UO$_2$ (cm^2)	Max. mol H$_2$O$_2$ produced from radiolysis (calc.)	Max. U dissolvable from reaction with H$_2$O$_2$ (µg)	U total dissolved measured (µg)	G_{eff}
Experiment 1: leach time 167 days						
1	–	2.59	5.3×10^{-7}	123	$17.8 \pm 3\%$	$0.145 \pm 3\%$
10	–	2.74	3.1×10^{-6}	739	$38.4 \pm 3\%$	$0.052 \pm 3\%$
100	–	2.65	1.9×10^{-5}	4570	$82.0 \pm 3\%$	$0.018 \pm 3\%$
1	+	2.88	5.7×10^{-7}	137	$214 \pm 5\%$	$1.56 \pm 5\%$
10	+	2.93	3.4×10^{-6}	790	$760 \pm 4\%$	$0.96 \pm 4\%$
100	+	2.53	6.6×10^{-5}	4370	$842 \pm 6\%$	$0.19 \pm 6\%$
Experiment 2: leach time 270 days						
1	–	3.10	9.9×10^{-7}	238	$30.5 \pm 8\%$	$0.128 \pm 8\%$
10	–	2.53	4.6×10^{-6}	1100	$38.9 \pm 7\%$	$0.035 \pm 7\%$
100	–	2.73	3.2×10^{-5}	7620	$62.7 \pm 6\%$	$0.008 \pm 6\%$
1	+	2.87	9.2×10^{-7}	220	$213 \pm 10\%$	$0.97 \pm 10\%$
10	+	2.69	4.9×10^{-6}	1170	$380 \pm 7\%$	$0.32 \pm 7\%$
100	+	3.08	3.6×10^{-5}	8590	$1280 \pm 11\%$	$0.15 \pm 11\%$

It is possible that the mixing of a very small quantity of [238]PuO$_2$ with a much larger quantity of UO$_2$ resulted in an inhomogeneous mixture, causing the observed discrepancies in the compositions of the materials.

The undoped material was mixed in a separate mill that had not been used in the preparation of the [238]Pu-doped materials. However, this second mill, although cleaned before use, must have contained traces of [238]Pu and [239+240]Pu because the undoped material contains a very small mass of [238]Pu and a somewhat larger mass of [239+240]Pu, for a total alpha-activity level of about 0.4 Ci/kg UO$_2$.

Previously published results from work with these materials [7,20] assumed the nominal compositions of 0, 1, 10 and 100 Ci/kg UO$_2$ to be correct, because actual compositions had not been measured and there was no obvious reason to suppose the target compositions were not reached. Although the numerical values previously reported [7,20] for some of the calculated parameters (e.g., G_{eff} and UERs) would be affected by using the nominal compositions rather than the actual compositions, this has no effect on the conclusions drawn from the results, because trends remain the same. In particular, the G_{eff} values reported in [20] need to be divided by factors of 2.2, 1.25 and 0.8, for the nominal 1, 10 and 100 Ci/kg UO$_2$ materials, respectively.

All calculations in the present paper have been performed using the actual compositions and activities of the [238]Pu-doped materials.

4.2. Dissolution experiments and dissolution rates

Fig. 1 shows the mass of U leached (in µg) from the UO$_2$ discs after 24 h, 176 d and 270 d. The 24 h pre-leach data (averaged for Experiments 1 and 2) are likely affected by rapid dissolution of any remaining fines and oxidized materials on the disc surfaces. There is a large difference in the amount of U dissolved in the 24 h pre-leach for solutions with and without carbonate. This suggests that either some of the underlying UO$_2$ matrix was dissolved by the carbonate-containing leachant or that not all oxidized material was removed by the carbonate-free leachant. Although we did not test this (e.g., by repeating the pre-leaching procedure several times), there are various arguments against the latter possibility.

Firstly, the rate of dissolution of any UO$_{2+x}$ oxidized layer on the discs is estimated to be, based on an expression developed by Bruno et al. [21], about 4.2 µg per day (at pH 9.5, assuming a geometric surface area of 2.6 cm^2). Fig. 1 shows that the amount of U dissolved by the carbonate-free leachant, in 24 h, exceeds 4.2 µg in two of the four cases. Furthermore, if these surfaces still contained considerable amounts of oxidized material after the 24 h pre-leach (i.e., amounts similar to that dissolved during the 24 h pre-leach in carbonate-containing solutions), one would expect (based on the estimated dissolution rate) that the amounts of U dissolved in the carbonate-free 167 d and 270 d tests would be considerably higher than measured (see Fig. 1). Secondly, if during the 24 h, 167 d and 270 d of leaching in carbonate-free waters only pre-oxidized materials were dissolving, one would not expect to observe any dependence on doping level. However, Fig. 1 shows that there is generally an increase in U release with increasing doping level for both carbonate-containing and carbonate-free solutions, suggesting an effect of radiolysis products on the UO$_2$ matrix.

Therefore, we conclude that, during the 24 h pre-leach, it is likely that all of the pre-oxidized layer and some of the underlying un-oxidized UO_2 matrix was dissolved by the carbonate-containing leachant and that most of the pre-oxidized layer was removed by the carbonate-free leachant.

Fig. 1 shows that for all doping levels, the total mass of U leached into solution is between 10 and 100 times larger in the solutions containing 0.1 M carbonate, than in the solutions without carbonate. Conversely, Fig. 2 shows that the mass of precipitated U on the surface of all discs is about 10 times lower in the presence of 0.1 M carbonate compared to the absence of carbonate. Both trends are the result of the faster U dissolution kinetics and the higher solubility of U in the 0.1 M carbonate solutions. Figs. 1 and 2 show that the amount of U dissolved or precipitated appears to generally increase with doping level, but that there is no consistent difference between the 167 d and 270 d results. One would expect the amount of U dissolved or precipitated to be larger after 270 d but this is not always the case.

Table 2 shows that dissolution rates ranged from 3.2×10^{-6} to 2.3×10^{-5} µg U/cm^2 s in carbonate solution and from 1.5×10^{-7} to 2.1×10^{-6} µg U/cm^2 s in carbonate-free solution. There appears to be a difference of only about a factor of 10 in dissolution rate for a 100-fold increase in doping level. A similar finding was reported by Rondinella et al. [8]. The influence of 0.1 M carbonate is more pronounced and appears to increase dissolution rates by 10 to almost 100 times over those measured in non-carbonate solutions (Fig. 1). This is due to the significant effects of carbonate on the kinetics and extent of UO_2 dissolution (Fig. 1), and possibly to the surface-sites blocking effects of precipitates in the absence of carbonate. Table 2 also shows that dissolution rates appear to be lower for the 270 d experiment than for the 167 d experiment. Although precipitation effects could be the cause of this decrease in carbonate-free solution, such precipitation is not expected to occur in 0.1 M carbonate solution. The decrease in dissolution rates over time in carbonate solution is, therefore, more likely an effect of initially accelerated dissolution at 'active' sites on the Pu-doped UO_2 surface, which are subsequently removed by dissolution. In carbonate-free solutions these 'active' sites dissolve as well initially but at a much slower rate than in carbonate solution, and precipitation at these 'active' sites will eventually block them, such that further dissolution is significantly suppressed.

4.3. Uranium enrichment ratios

Figs. 3 and 4 show UER's for the 167 d and 270 d experiments. In these figures, the UER's for the solution analysis, the surface analysis (from the 60 s acid dips) and the total system (solution + surface) analysis are shown. One would expect that the UER values for the total system should be 1, because it compares the total amounts of Pu and U dissolved in solution and remaining on the surface (either due to precipitation or to the unequal rates of Pu and U dissolution) to the composition of the doped material. That is, the UER's for the total system are in fact mass balance checks.

Fig. 3 shows that, for the 167 d experiment, in all but one case there is a considerable U enrichment in the leaching solutions, and in all cases a considerable Pu enrichment on the UO_2 surface, especially in 0.1 M carbonate. This suggests that U dissolves to a greater extent than Pu, particularly in the presence of 0.1 M carbonate. In the latter case, there appears to be a substantial Pu enrichment on the surface; but even in the absence of carbonate, there appears to be solution enrichment for U and some surface enrichment for Pu. The UER's for the total system show values close to one (0.75–0.97) for the experiments without carbonate, but values considerably larger than one (1.69–2.18) in the presence of carbonate. This suggests that in the experiments with 0.1 M carbonate some Pu is 'missing'.

Fig. 4 shows the same data for the 270 d experiment, essentially a duplicate experiment. Again, in all but one case there is considerable U enrichment in solution and in all cases there is Pu enrichment on the surface with total system UER's close to one (1.01–1.45) for the experiments without carbonate but considerably larger than one (1.51–1.89) in the presence of 0.1 M carbonate, suggesting again that some Pu is 'missing'.

A likely explanation for the 'missing' Pu is that, in the presence of 0.1 M carbonate, dissolution of U is extensive and rapid, and a relatively much smaller amount of Pu dissolves at the same time, producing a Pu-enriched surface layer. Further, the subsequent dissolution of the surface layer in 0.1 M HCl for 60 s likely did not dissolve all of the Pu left behind on the surface. This results in an apparent Pu deficit, as measured by the total system (solution + surface) UER. To remedy this, a stronger acid should have been used and/or a dissolution time longer than 60 s. It should be noted that, for a surface area of ~3 cm^2, dissolution of 300 µg of uranium (see Fig. 1) corresponds to the dissolution of a ~0.1 µm thick layer. Because this thickness is much smaller than the range of the alpha particles in the Pu-doped material (~12.4 µm [22]), the alpha dose at the solid/water interface should be relatively constant during the experiment. The alpha dose is determined by the volume of the Pu-doped UO_2 that can contribute to dose, and this volume is determined by the mean path length of alpha-particles in a UO_2 matrix (i.e., ~12.4 µm [22]).

In contrast, in the absence of carbonate, the total system UERs are approximately equal to 1. This suggests that U and Pu dissolve at somewhat similar rates under these conditions and any Pu precipitated on the surface

is likely co-precipitated with U(VI), which should dissolve easily and rapidly in 0.1 M HCl.

Figs. 3 and 4 show a remarkable deviation from the general pattern in the two experiments with the nominal 100 Ci/kg UO_2 material in the absence of carbonate. Whereas all other 10 experiments show an enrichment of U in solution and enrichment of Pu on the UO_2 surface, these two experiments show an enrichment of Pu in solution and either very little enrichment or in one case a small depletion of Pu on the surface. These two experiments were duplicates, in that they were carried out in identical solutions but with different discs of the nominal 100 Ci/kg Pu-doped UO_2 material. Therefore, these deviating patterns are likely real and not caused by a spurious effect of surface or material inhomogeneity. We speculate that the larger amount of PuO_2 in the nominal 100 Ci/kg UO_2 material has lead to radiation damage, especially in and near the PuO_2 islands, making these now more soluble than UO_2 in the absence of 0.1 M carbonate. We further speculate that in the presence of 0.1 M carbonate, the effects of carbonate on UO_2 dissolution kinetics and solubility still outweigh the proposed radiation-damage induced increase in PuO_2 solubility. Future studies will not include the 100 Ci/kg UO_2 material because of the possibility that the crystal lattice structure of this material is changing with time due to radiation damage caused by alpha decay.

4.4. G_{eff} values

The comparison of G_{eff} values for the 176 d and 270 d experiments in Table 3 shows lower G_{eff} values after 270 d, consistent with the observed decrease in dissolution rates over time. It further shows a significant reduction in G_{eff} values with increasing doping level. Assuming that these results are not affected by ingress of O_2 into the glass bottles or by the presence of pre-oxidized material (after the 24 h pre-leach), this suggests that, at the higher doping levels, the dissolution reaction becomes limited by the reaction rate between UO_2 and H_2O_2 and not by the production rate of H_2O_2. Intuitively, the overall dissolution reaction must become limited by the rate of production of H_2O_2 as the dose rate decreases.

The presence of 0.1 M carbonate inhibits uranium precipitation because of the higher solubility of U(VI) in such solutions. Table 3 shows a significant increase in the G_{eff} values in 0.1 M carbonate, consistent with the higher dissolution rates in carbonate solutions. This would suggest that precipitation results in lower G_{eff} values, possibly because the surface-blocking effect of precipitates leads to less UO_2 dissolution.

If there was no ingress of O_2 into the glass bottles and the radiolytically generated radical oxidants (OH, HO_2) contribute little to the oxidation of the UO_2 (i.e., the

radicals react before reaching the UO_2 surface), G_{eff} values should be less than 1. However, for the 167 d nominal 1 Ci/kg UO_2 experiment in 0.1 M carbonate, a G_{eff} value of 1.56 was measured. This suggests that UO_2 dissolution can also be caused by oxidants other than H_2O_2 (either ingressing O_2 or radiolytically produced radical oxidants). The effects of these minor oxidants would be more noticeable at the lower doping level, because at the higher doping levels the large production of H_2O_2 would 'swamp' any effects due to minor oxidants. Because, in the presence of carbonate, a significant amount of U was dissolved in the 24 h pre-leach (Fig. 1), it is not believed that the $G_{eff} > 1$ value is due to the dissolution of fines or pre-oxidized material.

It should be noted here that the absolute values of G_{eff} are strongly dependent on the actual doping levels of the materials. Although the bulk composition of the Pu-doped materials have been measured in this work, it is possible that the materials are inhomogeneous on a microscopic scale, in which case the composition of the surface region that contributes to dose in the dissolution experiments could deviate from the bulk composition. This could affect the absolute values of G_{eff} but it is not expected to change the very clear trend of decreasing G_{eff} values with increasing doping level. Therefore, the trends in the G_{eff} values in Table 3 are more suitable for validating the MPM predictions than the absolute values themselves.

Furthermore, for safety assessment purposes, G_{eff} values at very long times (>1000 years) are needed. Experiments over such long time periods are not feasible and other arguments and methods are needed to support the values of G_{eff} used in safety assessment calculations [23]. For example, the G_{eff} trends measured in this work could first be used in the validation of the MPM and then the MPM could be used to calculate G_{eff} values at long times.

4.5. Comparison with published uranium dissolution data for Pu-doped UO_2

Cobos et al. [24] and Rondinella et al. [9,25] have published U dissolution data obtained with Pu-doped materials that had similar doping levels to the nominal 10 Ci/kg UO_2 material used in our study. They used doped materials with a variety of surface areas, from fine-grained (particle size <63 μm) to course-grained (63 μm <particle size <125 μm) material and a variety of discs and pellets. Fig. 5 presents the cumulative amounts of uranium leached into solution as a function of time, obtained from these published studies and from our work, with all data normalized to surface area and all data obtained in carbonate-free solutions. Fig. 5 shows that our data agree quite well with the literature values, except perhaps for the data obtained with pellets. Thus, the dissolution data obtained in this work appear
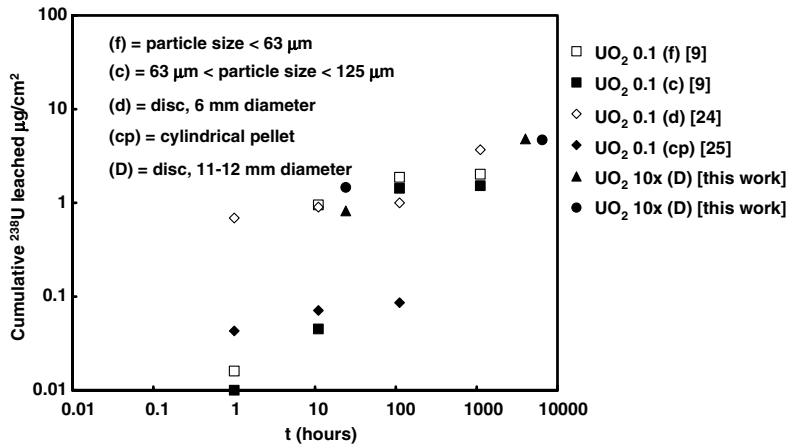
Fig. 5. Comparison of U leaching results in carbonate-free solutions (normalized for surface area) for the nominal 10 Ci/kg UO_2 material with published data for alpha-doped UO_2 with similar doping level.

to be consistent with published data for similar Pu-doped UO_2 materials.

4.6. Comparison with MPM predictions

The dissolution rates obtained in this work (Table 2) can be compared to MPM predictions of dissolution rates as a function of alpha-source strength. Fig. 6 compares the experimental dissolution rates in carbonate-free solution from our current study (plotted against alpha-source strength, calculated from the actual doping levels), and those derived from a study by King and Betteridge [3] who used external alpha-sources, with predictions from the MPM [26].

Since the MPM is a one-dimensional model, the experimental geometry can only be modelled approximately. In the MPM simulations, one boundary of the model is the surface of the dissolving solid and the other boundary is placed 0.01 cm away from this surface, where 0.01 cm is the estimated diffusion layer thickness for the experimental set-up [16]. At this latter boundary, chemical concentrations are set equal to those in the bulk solution. In particular, the concentration of H_2O_2, the only alpha-radiolysis product included in the MPM, is set to zero at this boundary.

Two curves are shown in Fig. 6 for the MPM, corresponding to two possible values for the electrochemical rate constant for the anodic dissolution of UO_2 as
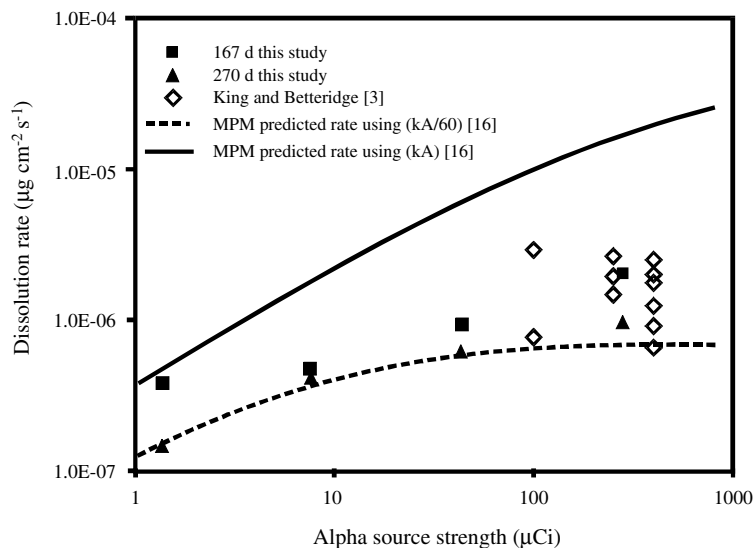

Fig. 6. Comparison of experimental dissolution rates as a function of alpha source strength in carbonate-free solution with predictions from the MPM model.

UO_2^{2+}, i.e., 5×10^{-12} mol/cm^2 s (kA) and 8×10^{-14} mol/cm^2 s (kA/60) [16], where the lower value was derived from experimental data and the higher value attempts to compensate for film-formation effects [10]. The experimental data fall within the range of dissolution rates predicted by the MPM for these two kA values but appear to agree better with the curve obtained using the lower rate constant. The dissolution rates obtained here have provided an independent verification of MPM predictions over the time frame of the experiments.

5. Summary and conclusions

Dissolution experiments were performed with ^{238}Pu-doped UO_2 materials ranging in nominal doping levels from about 1 to 100 Ci/kg UO_2 (actual doping levels 0.4–80 Ci/kg UO_2). The experiments were carried out in both 0.1 M NaClO$_4$ and 0.1 M NaClO$_4$ + 0.1 M carbonate at pH 9.5. The purpose of these experiments was to investigate the effects of alpha dose-rate on UO_2 dissolution and to obtain UO_2 dissolution rates and G_{eff} values as a function of alpha dose rate. The measured dissolution rates and G_{eff} values could then be used in the validation of the Mixed Potential Model (MPM) for used UO_2 fuel dissolution, a detailed (electrochemical) mechanistic model developed to predict the long-term dissolution of used fuel.

Experimental results suggest a complicated simultaneous effect of carbonate and radiolysis on U and Pu dissolution and precipitation. In the absence of carbonate, a precipitate (slightly enriched in Pu) appears to form, which could block dissolving surface sites, resulting in a decrease in UO_2 dissolution. In the presence of carbonate, ^{238}Pu appears to become enriched substantially on the UO_2 surface, likely due to the accelerated dissolution of uranium, relative to plutonium, in carbonate solution.

Dissolution rates increased with doping level and ranged from 3.2×10^{-6} to 2.3×10^{-5} µg U/cm^2 s in carbonate solution and from 1.5×10^{-7} to 2.1×10^{-6} µg U/cm^2 s in NaClO$_4$ solution. Dissolution rates increased by only about 10 times for a 100-fold increase in doping level, but increased between 10 and 100 times in 0.1 M carbonate, compared to dissolution rates in carbonate-free solution. Dissolution rates appeared to decrease with time, possibly as a result of initially accelerated dissolution at 'active' sites on the ^{238}Pu-doped UO_2 surfaces, which are subsequently either blocked by precipitates (in carbonate-free solutions) or removed by dissolution (in carbonate solutions).

Measured G_{eff} values ranged from 0.008 to 1.56 and increased with decreasing doping levels. If these results were not affected by ingress of O$_2$ into the glass bottles or by the presence of pre-oxidized material (after the 24 h pre-leach), this suggests that the dissolution reac-

tion is limited by the reaction rate between UO_2 and H_2O_2 at high dose rates, but becomes increasingly limited by the rate of production of H_2O_2 (or other radiolytically produced oxidants) at lower dose rates. G_{eff} values also appeared to decrease over time, as a consequence of the observed decrease in dissolution rates. G_{eff} values increase in the presence of carbonate, possibly indicating that precipitation in the absence of carbonate results in surface-site blocking effects.

Measured uranium release data, normalized to surface area, are similar to published data obtained by others with Pu-doped UO_2 of similar doping levels. Finally, measured dissolution rates fall within the predictions of the MPM, providing an independent validation of the MPM over the time frame of the experiments.

References

[1] D.W. Shoesmith, Fuel corrosion processes under waste disposal conditions. Atomic Energy of Canada Limited Report, AECL-12034, 1999.

[2] S. Sunder, D.W. Shoesmith, N.H. Miller, J. Nucl. Mater. 244 (1997) 66.

[3] F. King, J.S. Betteridge, The effect of α-radiolysis on the oxidative dissolution of UO_2 under strongly oxidizing conditions. Ontario Power Generation, Nuclear Waste Management Division Report 06819-REP-01200-10006-R00, 1999. Toronto, Ontario.

[4] D.W. Shoesmith, S. Sunder, J.S. Betteridge, The influence of alpha-radiolysis on UO_2 fuel dissolution as observed in electrochemical experiments. Ontario Power Generation, Nuclear Waste Management Division Report 06819-REP-01200-10047-R00, 2000. Toronto, Ontario.

[5] D.W. Shoesmith, W.H. Hocking, S. Sunder, J.S. Betteridge, N.H. Miller, The electrochemistry of hydrogen peroxide on UO_2 electrodes and the influence of hydrogen peroxide on the corrosion of UO_2. Ontario Power Generation, Nuclear Waste Management Division Report 06819-REP-01200-10050-R00, 2001. Toronto, Ontario.

[6] S. Stroes-Gascoyne, F. King, J.S. Betteridge, The effects of alpha-radiolysis on UO_2 dissolution determined from preliminary electrochemical experiments with ^{238}Pu-doped UO_2. Ontario Power Generation, Nuclear Waste

Management Division Report 06819-REP-01300-10030-R00, 2002a. Toronto, Ontario.

[7] S. Stroes-Gascoyne, F. King, J.S. Betteridge, F. Garisto, Radiochim. Acta 90 (2002) 603.

[8] V.V. Rondinella, Hj. Matzke, J. Cobos, T. Wiss, Mater. Res. Soc. Symp. Proc. 556 (1999) 447.

[9] V.V. Rondinella, Hj. Matzke, J. Cobos, T. Wiss, Radiochim. Acta 88 (2000) 527.

[10] D.W. Shoesmith, F. King, A mixed-potential model for the prediction of the effects of alpha-radiolysis, precipitation and redox processes on the dissolution of used nuclear fuel. Ontario Hydro, Nuclear Waste Management Division Report 06819-REP-01200-0038-R00, 1998.

[11] L.H. Johnson, D.M. LeNeveu, F. King, D.W. Shoesmith, M. Kolar, D.W. Oscarson, S.Sunder, C. Onofrei, J.L. Crosthwaite, The disposal of Canada's nuclear fuel waste: A study of postclosure safety of in-room emplacement of used CANDU fuel in copper containers in permeable plutonic rock, vol. 2: vault model. Atomic Energy of Canada Limited Report, AECL-11494-2, COG-96-552-2, 1996.

[12] F. King, M. Kolar, Prediction of the effects of a-radiolysis, precipitation and redox reactions with Fe and Fe(II) on the dissolution of UO_2 using the mixed-potential model of fuel dissolution (MPM version 1.1). Ontario Power Generation, Nuclear Waste Management Division Report 06819-REP-01200-10014, 1999. Toronto, Ontario.

[13] F. King, M. Kolar, Analysis of the effect of cladding on the oxidative dissolution of used nuclear fuel using the mixed potential model of fuel dissolution (MPM Version 1.2). Ontario Power Generation, Nuclear Waste Management Division Report 06819-REP-01200-10022, 2000. Toronto, Ontario.

[14] F. King, M. Kolar, Mixed potential model simulations of the effects of porous film formation on the dissolution of used fuel (MPM Version 1.3). Ontario Power Generation, Nuclear Waste Management Division Report 06819-REP-01300-10019-R00, 2001a. Toronto, Ontario.

[15] F. King, M. Kolar, An improved C-steel corrosion model for the mixed-potential model for used fuel dissolution (MPM Version 1.4). Ontario Power Generation, Nuclear

Waste Management Division Report 06819-REP-01300-10027-R00, 2001b. Toronto, Ontario.

[16] F. King, M. Kolar, Validation of the mixed-potential model for used fuel dissolution against experimental data. Ontario Power Generation, Nuclear Waste Management Division Report 06819-REP-01200-10077-R00, 2002a. Toronto, Ontario.

[17] F. King, M. Kolar, Sensitivity analysis of the factors affecting the effective G-value G_{eff} in the mixed-potential model for used fuel dissolution. Ontario Power Generation, Nuclear Waste Management Division Report 06819-REP-01300-10044-R00, 2002b. Toronto, Ontario.

[18] S. Stroes-Gascoyne, J.S. Betteridge, F.C. Dimayuga, F.B. Gravelle, K.P. Doering, Preparation and testing of [238]Pu-doped electrodes for use in electrochemical studies of UO_2 dissolution. Ontario Power Generation, Nuclear Waste Management Division Report 06819-REP-01200-10037-R00, 2000. Toronto, Ontario.

[19] S. Sunder, N.H. Miller, D.W. Shoesmith, Corros. Sci. 46 (2004) 1095.

[20] S. Stroes-Gascoyne, J.S. Betteridge, Mater. Res. Soc. Symp. Proc. 824 (2004) 175.

[21] J. Bruno, I. Casas, I. Puigdomenech, Geochim. Cosmochim. Acta 55 (1991) 647.

[22] F. Garisto, Annu. Nucl. Energy 16 (1989) 33.

[23] L.H. Johnson, P.A. Smith, The interaction of radiolysis products and canister corrosion products and the implications for spent fuel dissolution and radionuclide transport in a repository for spent fuel. NAGRA Technical Report NTB 00-04, Switzerland, 2000.

[24] J. Cobos, Hj. Matzke, V.V. Rondinella, T. Wiss, A. Martinez-Esparza, Alpha-radiolysis effects on UO_2 dissolution, in: Global '99, International Conference on Future Nuclear Systems Jackson Hole, WY, 1999.

[25] V.V. Rondinella, J. Cobos, H. Matzke, T. Wiss, P. Carbol, D. Solatie, Mater. Res. Soc. Symp. Proc. 663 (2001) 391.

[26] S. Stroes-Gascoyne, J.S. Betteridge, The effects of alpha-radiolysis on UO_2 dissolution determined from batch experiments with [238]Pu-doped UO_2. Ontario Power Generation, Nuclear Waste Management Division Report 06819-REP-01200-10110-R00, 2003. Toronto, Ontario.